*The 2013 World Congress on*
***Advances in Structural Engineering and Mechanics (ASEM13)***
*Jeju, Korea, September 8-12, 2013*

# Evaluation of rotational displacements of masonry walls of castles subjected to dynamic horizontal loading

* Takeshi Masui[1)], Yasutaka Hiroishi[2)] and Yuji Oshima[2)]

[1), 2)] *Department of Architecture, Kansai University, Suita, Osaka 564-8680, Japan*
[1)] *masui@kansai-u.ac.jp*

## ABSTRACT

We develop a method to quantitatively evaluate the amount of rotational displacement of masonry walls subjected to dynamic horizontal loading. Shaking table tests using a gravity retaining wall model are performed to confirm the validity of the method. As the calculated rotational displacements of the model show good agreement with those of the test results, validity of the method for predicting rotational displacements of the walls is clarified.

## 1. INTRODUCTION

Japan has a number of existing masonry walls of castles that are valuable cultural assets more than 400 years after their construction, although some are partially collapsed and damaged. Recently, masonry walls have been attracting attention as a valuable historical and cultural heritage, which has spurred interest in stone restoration techniques.

Earthquakes are mentioned as a major cause of damage to masonry walls that have collapsed. For example, the masonry walls of Komine castle in Fukushima prefecture collapsed due to Tohoku Region Pacific Coast Earthquake that occurred on 11 March 2011. Although it is desirable that masonry wall restoration work should be principally based on traditional techniques, conformity to contemporary Japanese building codes is also required for the assessment of restored structures, but traditional masonry skills are difficult to assess according to contemporary codes. This has often led to an underestimation of ancient skills, or restoration work performed without the application of appropriate safety standards. Thus, it is useful to explore how the principles of current scientific techniques can be used to interpret ancient masonry techniques, and clarify the relationships between these and modern techniques.

Masonry wall model tests conducted by Masui and Yao (2007) and Matsunaga, Masui and Yao (2008) confirmed that collapse shapes can be categorized into three patterns as shown in Fig. 1. The masonry wall is composed of a foundation stone and upper part stones. A rocking represents a rotation of the upper part stones on the

[1)] Associate Professor
[2)] Graduate Student

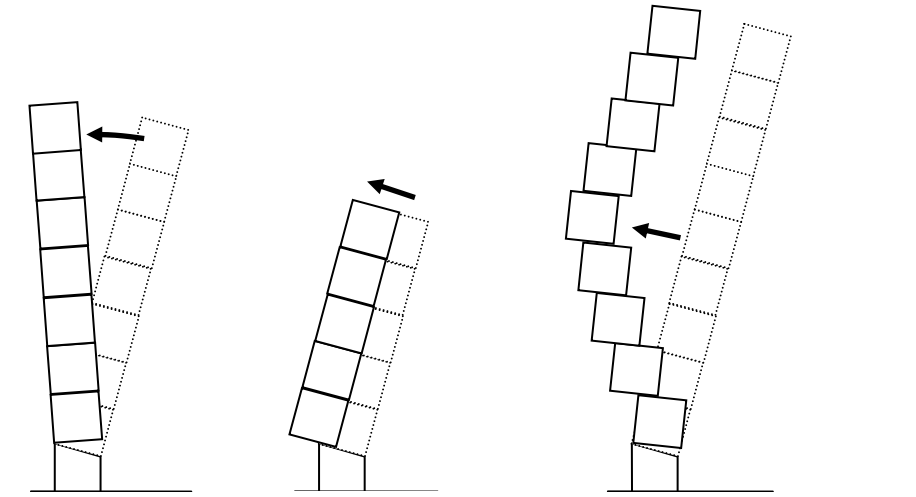


Fig. 1 Collapse shapes of a masonry wall

foundation stone. A sliding represents a parallel displacement of the upper part stones on a surface plane of a foundation stone. The third collapse shape is called “combined rocking & sliding”.

Even if masonry walls were deformed by earthquakes, they do not reach the collapse if the deformation remained below a certain level because they have ability of absorption energy by deforming. In brief masonry walls have three states that are stable state without deformation, stable state after deforming and collapsed state. This is one characteristic of masonry walls. Thus, to develop masonry wall design criteria, it is necessary to quantitatively evaluate the amount of energy that a wall can absorb during earthquake.

We are making researches on the stone wall in stages for each collapse shapes. Hiroishi,Y., Masui,T. and Yao,S. (2012) made the research that focuses on only sliding collapse shape. In the study, we developed a method to quantitatively evaluate the amount of horizontal displacement of masonry walls subjected to dynamic horizontal loading. Shaking table tests using a gravity retaining wall model have performed to confirm the validity of the method. As the calculated horizontal displacements of the model show good agreement with those of the test results, validity of the theory for predicting horizontal displacements of the walls is clarified. Masui, T. and Hiroishi, Y. (2012) developed a method for evaluating the amount of energy that a masonry wall can absorb during an earthquake, based on the amount of masonry wall sliding caused by an input acceleration that exceeds a critical degree of sliding acceleration. An index was proposed for the seismic performance of a masonry wall corresponding to the wall’s capacity to absorb energy during earthquake.

In this paper, we develop a method to quantitatively evaluate the amount of rotational displacement subjected to dynamic horizontal loading. We confirm the validity of the method in shaking table tests using a small model. We deal with the structural mechanics of the masonry wall section that represents the main part of the masonry wall structure, excluding corners.

## 2. METHOD TO EVALUATE THE AMOUNT OF ROTATIONAL DISPLACEMENT

*2.1 Analysis Model*

We assume the upper part stones behave as a rigid body acting just upon the foundation stone. We are modeling the upper part stones into a stone wall. The components of the analysis model are the stone wall, the foundation stone and backfill soil. Backfill soil is assumed to be sandy soil with cohesion = 0 and have a horizontal surface. Fig. 2 illustrates a sectional view of the stone wall with height $H$ built on a straight slope line to form angle $\theta$ between the horizontal plane and the stone wall, and $b$ represents the wall thickness. $g$ is acceleration of gravity. $L$ is length of the upper stone. $m_s$ is mass of the stone wall. $I_s$ is moment of inertia of the stone wall. The soil wedge is formed by the plastic slip line of the backfill soil. It is assumed that the stone wall will move only by rocking around the point O without sliding (Hiroishi, Y., Masui, T. and Yao, S. 2013). $m_w$ is mass of the soil wedge. $P_r$ is the active earth pressure during earthquake. $R$ is the reaction force that the soil wedge receives from backfill soil. $N$ and $Q$ are the axial and frictional forces at the bottom of the stone wall.

When the ground excited at absolute acceleration $\ddot{X}$ in the forward direction (direction from the stone wall toward the backfill soil), the stone wall will move at angular acceleration $\ddot{\beta}$, horizontal relative acceleration $\ddot{x}_s$ and vertical relative acceleration $\ddot{y}_s$.

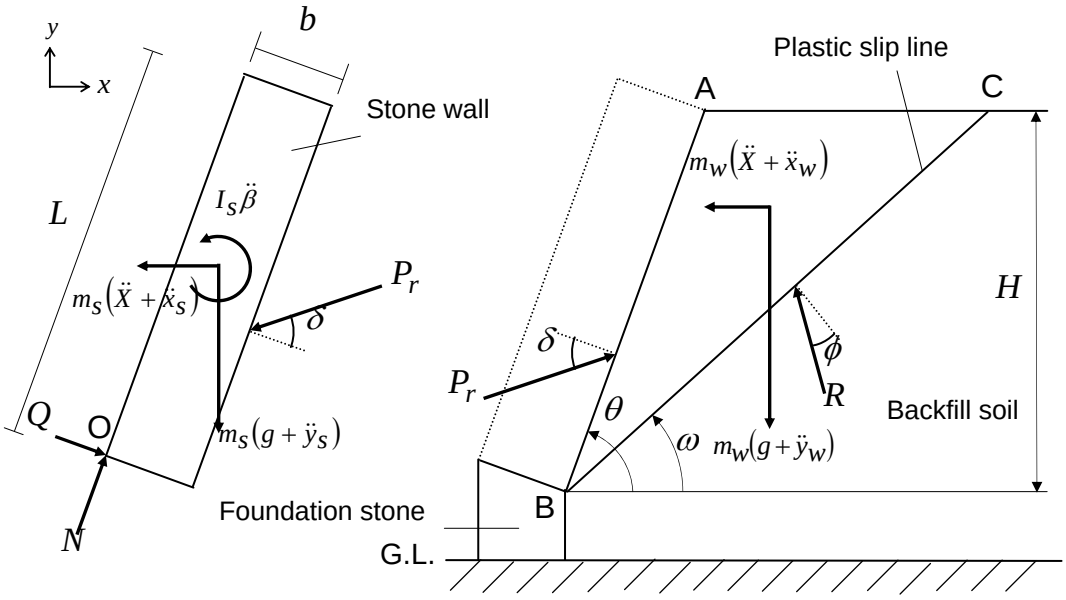


Fig. 2 Masonry wall analysis model considering rocking during earthquake

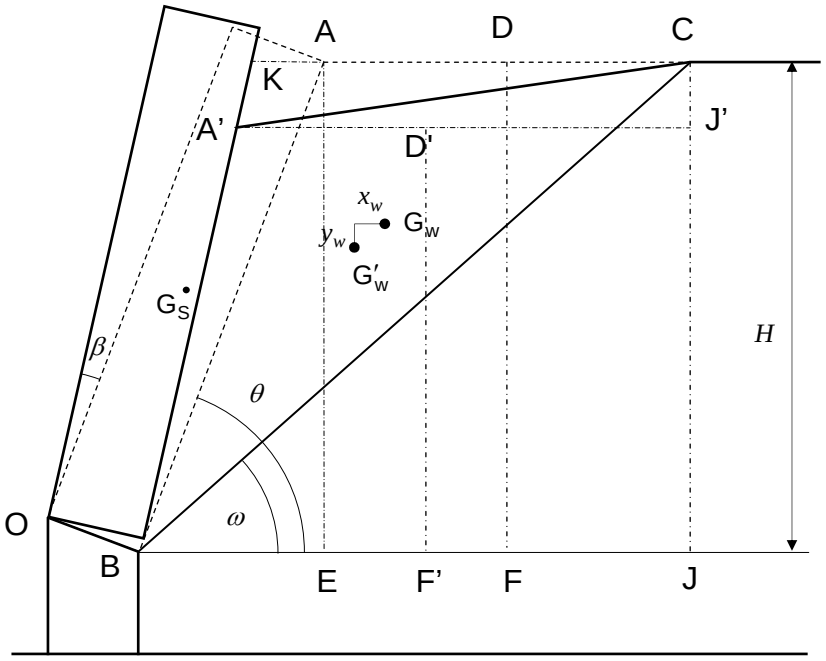


Fig. 3 Deformed configuration of the soil wedge

We carried out preliminary shaking table tests to grasp characteristics of the behavior of the soil wedge when the stone wall is rocking. As a result of the observation, we adopted a deformed configuration of the soil wedge as an analysis model as shown in Fig.3. △ABC and △A'BC represent initial and deformed shapes of the soil wedge, respectively. We assume that areas of both triangles are identical. We also assume that energy of the shape change is small and negligible compared with energy of a rigid body displacement of soil wedge. We take into account the influence of the shape change for compatibility conditions between the stone wall displacement and the soil wedge displacement. Inertial forces of the soil wedge can be represented by accelerations of the center of gravity of the soil wedge $G_w$ only. The center of gravity of the soil wedge will move at horizontal relative acceleration $\ddot{x}_w$ and vertical relative acceleration $\ddot{y}_w$.

*2.2 Critical Rocking Acceleration*

Eq. (1) and Eq. (2) can be obtained from the equilibrium of forces acting on the stone wall in the horizontal and vertical directions, respectively:

$$m_s(\ddot{X} + \ddot{x}_s) = -P_r \sin(\theta + \delta) + Q \sin\theta + N \cos\theta, \quad (1)$$

$$m_s(g + \ddot{y}_s) = P_r \cos(\theta + \delta) - Q \cos\theta + N \sin\theta, \quad (2)$$

where $\delta$ is the friction angle between the backfill soil and the stone wall.

Eqs. (3) ~ (5) can be obtained from the equilibrium of forces acting on the stone

wall in the rotational direction:

$$I_s\ddot{\beta} = \frac{L}{2}Q - \frac{b}{2}N - P_r L_P\,, \tag{3}$$

$$I_s = \frac{m_s}{12}\left(b^2 + L^2\right), \tag{4}$$

$$L_P = \left(\frac{L}{2} - \frac{H}{3\sin\theta}\right)\cos\delta + \frac{b}{2}\sin\delta\,. \tag{5}$$

When rotational angle $\beta$ is small, the compatibility conditions can be obtained from the assumption to the stone wall movement as follows:

$$\ddot{x}_s = -\frac{\sqrt{b^2 + L^2}}{2}\ddot{\beta}\cos\theta\,, \tag{6}$$

$$\ddot{y}_s = \frac{\sqrt{b^2 + L^2}}{2}\ddot{\beta}\sin\theta\,. \tag{7}$$

Eq. (8) and Eq. (9) can be obtained from the equilibrium of forces acting on the soil wedge in the horizontal and vertical directions, respectively:

$$m_w(\ddot{X} + \ddot{x}_w) = P_r\sin(\theta + \delta) - R\sin(\omega - \phi)\,, \tag{8}$$

$$m_w(g + \ddot{y}_w) = -P_r\cos(\theta + \delta) + R\cos(\omega - \phi)\,, \tag{9}$$

where $\phi$ is the internal friction angle of the backfill soil and $\omega$ is the angle between the plastic slip line and the horizontal plane.

Eqs. (10) ~ (12) can be obtained from the assumption of the soil wedge deformation:

$$\triangle KBA = \triangle KA'C, \tag{10}$$

$$\triangle KBA = \frac{1}{2}\overline{KB}\cdot\overline{AB}\sin\beta\,, \tag{11}$$

$$\triangle KA'C = \frac{1}{2}\overline{KC}\cdot\overline{CJ'}\,. \tag{12}$$

D ~ J' are shown in Fig .3 where D is the midpoint of the line segment AC.

Eqs. (13) ~ (15) can be obtained by a geometrical consideration of the soil wedge deformation:

$$x_w = \frac{2}{3}\overline{BF} - \frac{\overline{BJ}}{3}\cdot\frac{\overline{CJ'}}{H} - \frac{2}{3}\overline{BF'}\,, \tag{13}$$

$$y_w = \frac{\overline{CJ'}}{3}\,, \tag{14}$$

$$\beta = \frac{3\overline{\mathrm{AC}} y_w \sin\theta}{\overline{\mathrm{AB}}\left(H - 3y_{\mathrm{w}}\right) - 3\overline{\mathrm{AC}} y_w \cos\theta}. \tag{15}$$

Since a relation between $x_w$ and $y_w$ is almost linear and that between $y_w$ and $\beta$ is also almost linear, linear approximations by applying Taylor expansion to the relations lead Eqs. (16) ~ (19).

$$\beta = D_1 y_w, \tag{16}$$

$$x_w = D_2 y_w, \tag{17}$$

where

$$D_1 = -\frac{3\sin\theta}{L\tan\omega}, \tag{18}$$

$$D_2 = \frac{\sin(\theta - \omega)}{\sin\theta\sin\omega}. \tag{19}$$

Let denote $\overline{\mathrm{OA_H}}$ and $\overline{\mathrm{OA_V}}$ as horizontal and vertical components of $\overline{\mathrm{OA}}$ respectively. Solving the above equations simultaneously, the active earth pressure $P_r$ during earthquake considering the rocking can be obtained as follows:

$$P_r = \frac{B_1\ddot{X} + B_2 g}{B_3 m_s - B_4 m_w} m_s m_w, \tag{20}$$

where

$$B_1 = \overline{\mathrm{OG_S}} B_5 D_1 \cos(\omega - \phi) - 3\overline{\mathrm{OA_H}} B_6 b, \tag{21}$$

$$B_2 = \overline{\mathrm{OG_S}} B_5 D_1 \sin(\omega - \phi) + 3\overline{\mathrm{OA_V}} B_6 b, \tag{22}$$

$$B_3 = \overline{\mathrm{OG_S}} B_5 D_1 \sin(\theta + \delta - \omega + \phi) + 3B_6 b\overline{\mathrm{OA_V}}, \tag{23}$$

$$B_4 = 3B_6 B_7, \tag{24}$$

$$B_5 = \overline{\mathrm{OA_V}}\left(2\overline{\mathrm{OG_S}} - 3b\right)\cos\theta - \overline{\mathrm{OA_H}}\left(2\overline{\mathrm{OG_S}} + 3b\right)\sin\theta, \tag{25}$$

$$B_6 = D_2\cos(\omega - \phi) + \sin(\omega - \phi), \tag{26}$$

$$B_7 = \overline{\mathrm{OA_H}}\left\{2L_P\sin\theta - b\cos(\theta + \delta)\right\} - \overline{\mathrm{OA_V}}\left\{2L_P\cos\theta + b\sin(\theta + \delta)\right\}. \tag{27}$$

$\omega$ is determined by the condition of maximization of Eq. (28),

$$\frac{dP_r}{d\omega} = 0. \tag{28}$$

Angular acceleration $\ddot{\beta}$ can be obtained as follows:

$$\ddot{\beta} = \frac{D_1\left\{P_r\sin(\theta + \delta - \omega + \phi) - m_w\ddot{X}\cos(\omega - \phi) - m_w g\sin(\omega - \phi)\right\}}{m_w\left\{D_2\cos(\omega - \phi) + \sin(\omega - \phi)\right\}}. \tag{29}$$

The state when $\ddot{\beta} = 0$ is called the critical rocking state of the stone wall, and in this state, $\ddot{X}_{cr}$ is the critical rocking acceleration, and $P_{cr}$ is the active earth pressure during the critical rocking state. Eqs. (30) ~ (34) can be obtained from the equilibrium of forces acting on the stone wall and the soil wedge in the horizontal and vertical directions, respectively:

$$m_s \ddot{X}_{cr} = -P_{cr} \sin(\theta + \delta) + Q \sin\theta + N \cos\theta , \tag{30}$$

$$m_s g = P_{cr} \cos(\theta + \delta) - Q \cos\theta + N \sin\theta , \tag{31}$$

$$0 = \frac{L}{2} Q - \frac{b}{2} N - P_{cr} L_P , \tag{32}$$

$$m_w \ddot{X}_{cr} = P_{cr} \sin(\theta + \delta) - R \sin(\omega - \phi), \tag{33}$$

$$m_w g = -P_{cr} \cos(\theta + \delta) + R \cos(\omega - \phi). \tag{34}$$

Solving Eqs. (30) ~ (34) simultaneously, $\ddot{X}_{cr}$ and $P_{cr}$ can be obtained as follows.

$$\ddot{X}_{cr} = \frac{\overline{\mathrm{OA_H}} m_s \sin(\theta + \delta - \omega + \phi) - (L\cos\delta - b\sin\delta - 2L_P) m_w \sin(\omega - \phi)}{\overline{\mathrm{OA_V}} m_s \sin(\theta + \delta - \omega + \phi) + (L\cos\delta - b\sin\delta - 2L_P) m_w \cos(\omega - \phi)} g , \tag{35}$$

$$P_{cr} = \frac{\ddot{X}_{cr} \cos(\omega - \phi) + g \sin(\omega - \phi)}{\sin(\theta + \delta - \omega + \phi)} m_w . \tag{36}$$

*2.3 Amount of Rocking Displacement Considering Stone Wall rotation*

The stone wall rotates when the input acceleration exceeds the critical rocking acceleration $\ddot{X}_{cr}$. Here, we focus on a single acceleration input to the stone wall, whose value is greater than that of the critical rocking acceleration. $t_{k1}$ is the time when $\ddot{X}$ exceeds $\ddot{X}_{cr}$ and $t_{k2}$ is the time when $\ddot{X}$ becomes less than $\ddot{X}_{cr}$. $t_{k3}$ is the time when the rotational velocity of the stone wall with respect to the ground is zero. In $t_{k1} \le t \le t_{k2}$, the relative acceleration of the stone wall $\ddot{\beta}_k$ can be represented as Eq. (37) by transforming Eq. (29). In $t_{k2} \le t \le t_{k3}$, the value of $\ddot{X}$ in Eq. (29) is 0 and the active earth pressure is assumed to be the active earth pressure in the stationary state $P_a$. The rotational acceleration of the stone wall $\ddot{\beta}_a$ is calculated by Eqn. (38).

$$\ddot{\beta}_k = \frac{D_1 \left\{ P_{cr} \sin(\theta + \delta - \omega + \phi) - m_w \ddot{X} \cos(\omega - \phi) - m_w g \sin(\omega - \phi) \right\}}{m_w \left\{ D_2 \cos(\omega - \phi) + \sin(\omega - \phi) \right\}} , \tag{37}$$

$$\ddot{\beta}_a = \frac{D_1 \left\{ P_a \sin(\theta + \delta - \omega + \phi) - m_w g \sin(\omega - \phi) \right\}}{m_w \left\{ D_2 \cos(\omega - \phi) + \sin(\omega - \phi) \right\}} . \tag{38}$$

The amount of the rotational displacement is obtained by integrating the relative velocity $\dot{\beta}$ during $t_{k1} \le t \le t_{k3}$ with respect to time. The total amount of the rotational displacement is evaluated by iterating this procedure (Newmark 1965).

## 3. SHAKING TABLE TESTS OF GRAVITY RETAINING WALL MODEL

### *3.1. Outline*

We carried out shaking table tests using a gravity retaining wall model as the upper part stones to confirm the validity of evaluation method of amount of rotational displacement of the upper part stones. Input wave is sine wave in horizontal direction. The tests were performed in 8 cases with different test conditions by the combination of two angles of slopes of the wall, two frequencies of input waves and two aspect ratios $L/b$.

### *3.2. Specimens*

The wall is composed of three parts which are upper central part walls and upper both ends walls and a foundation stone as shown in Fig. 4 and Fig. 5. The mass of the wall stones per unit volume are $\rho_s = 2.20\,\mathrm{g/cm^3}$. Model size of upper part walls is shown in Table 1.

Backfill soil consists of dry sand. Soil particle density of backfill soil is $\rho = 2.65\,\mathrm{g/cm^3}$. The bulk density of back soil is $\rho_b = 1.49\,\mathrm{g/cm^3}$. This corresponds to relative density as $54\%$. Internal friction angle of backfill soil is $\phi = 38.2^\circ$ from three times results of the triaxial compression experiments regarded relative density as $54\%$ under confining pressures as 50, 100, 200kPa.

Since there is no standard experiment method about friction angle of the upper part walls and the backfill soil, we carried out measurement tensile tests of friction coefficient by a self-made equipment. Friction angle $\delta$ between the upper part walls and the backfill soil is obtained as $\delta = 22.8^\circ \sim 26.6^\circ$.

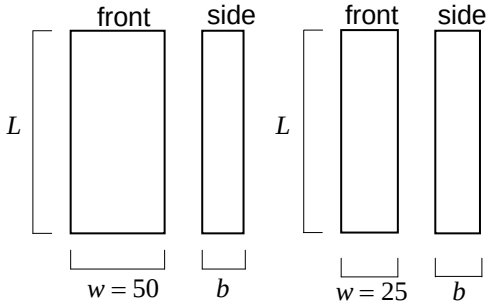


Fig. 4 Upper part walls (mm)

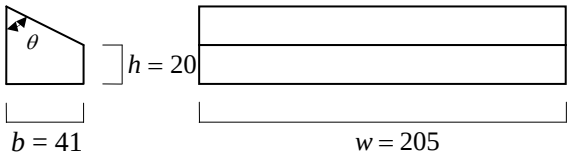


Fig. 5 A foundation stone (mm)

Table 1 Model size

| $\theta$ | 80° | | 82° | |
|---|---|---|---|---|
| $L/b$ | 5 | 7 | 5 | 7 |
| $b$ [mm] | 24 | 17 | 24 | 17 |
| $L$ [mm] | 120 | 119 | 120 | 119 |

*3.3. Shaking table test model*

Fig. 6 shows the experimental equipment. Shaking table test are performed in following manner:

1) The foundation stone corresponding to the designated slope angle is fixed on the bottom plate of experimental equipment.
2) The upper part walls are placed on the surface of the foundation stone and fill backfill soil to be the gravity sediment state.
3) The input waves are applied in horizontal direction. The amplitudes of the input waves are set to be slightly higher than the theoretically predicted values of the critical rocking accelerations.
4) Horizontal displacements of the wall on the vibration table are measured by laser displacement sensors.

Parameters of Input waves are shown in Table 2 and Table 3.

*3.4. Results*

Fig.7~14 show comparisons between experimental results and analysis results.

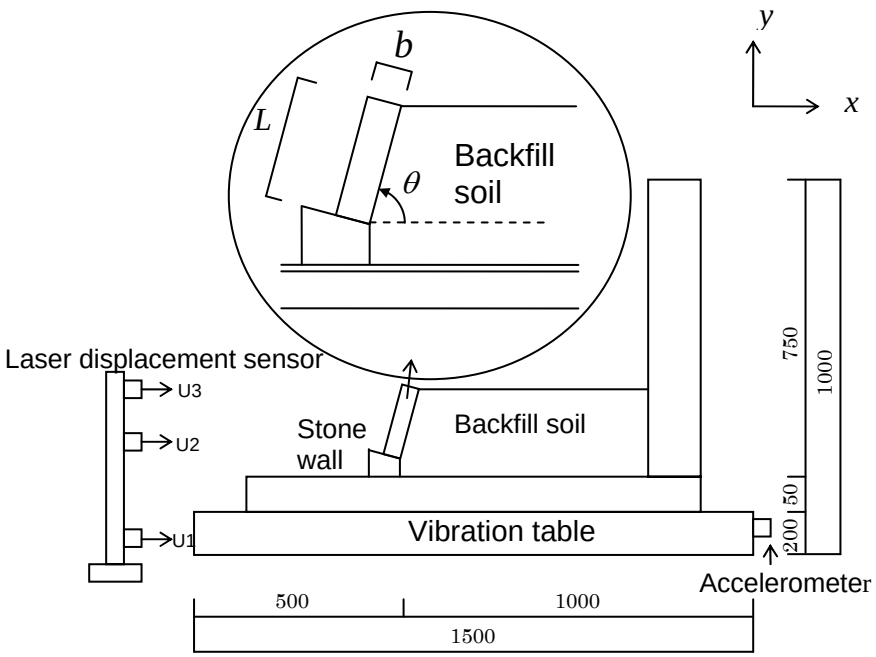


Fig. 6 Shaking table test model (mm)

Table 2 Input wave ($L/b = 5$)

| $\theta$ | 80° | | 82° | |
|---|---|---|---|---|
| Frequency [Hz] | 3.0 | 6.0 | 3.0 | 6.0 |
| Amplitude [mm] | 6.2 | 1.3 | 5.4 | 1.2 |

Table 3 Input wave ($L/b = 7$)

| $\theta$ | 80° | | 82° | |
|---|---|---|---|---|
| Frequency [Hz] | 3.0 | 6.0 | 3.0 | 6.0 |
| Amplitude [mm] | 3.2 | 0.7 | 1.9 | 0.6 |

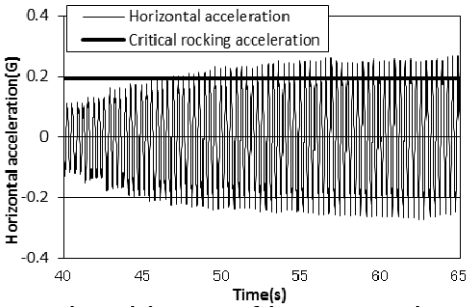


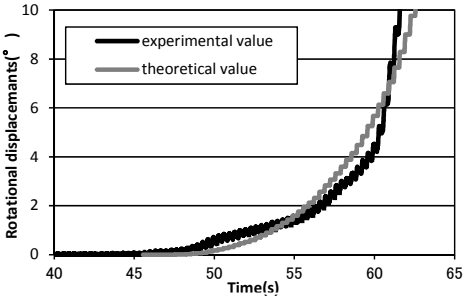


(a)Time history of input accelerations (b)Rotational displacements

Fig .7 Comparisons between experimental value and theoretical value

$(L/b=5,\theta=80°,3\text{Hz},\delta=25.5°)$

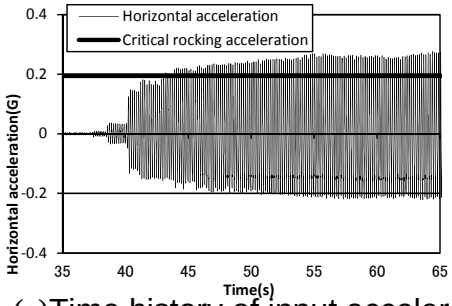


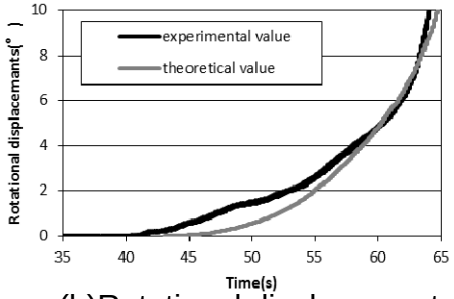


(a)Time history of input accelerations (b)Rotational displacements

Fig .8 Comparisons between experimental value and theoretical value

$(L/b=5,\theta=80°,6\text{Hz},\delta=25.5°)$

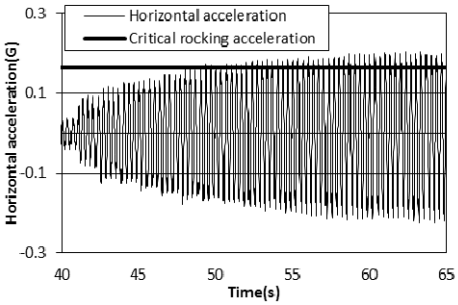


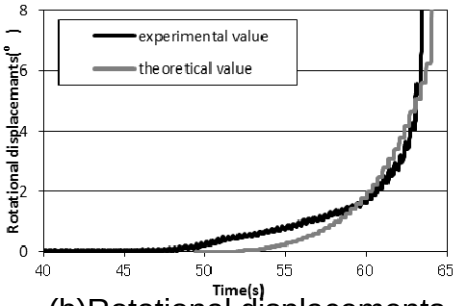


(a)Time history of input accelerations (b)Rotational displacements

Fig .9 Comparisons between experimental value and theoretical value

$(L/b=5,\theta=82°,3\text{Hz},\delta=26.4°)$

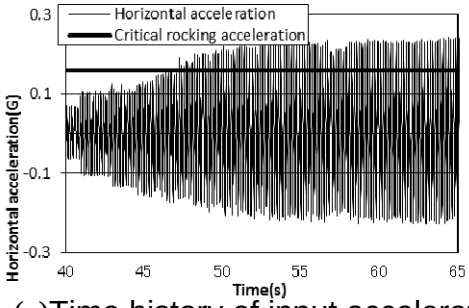


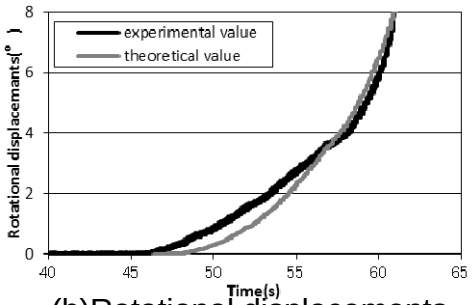


(a)Time history of input accelerations (b)Rotational displacements

Fig .10 Comparisons between experimental value and theoretical value

$(L/b=5,\theta=82°,6\text{Hz},\delta=25.0°)$

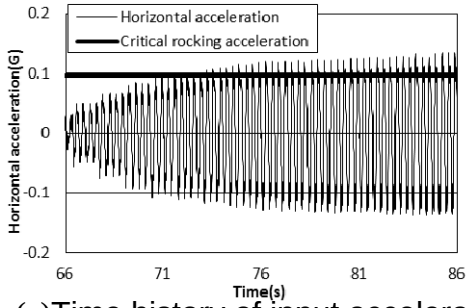


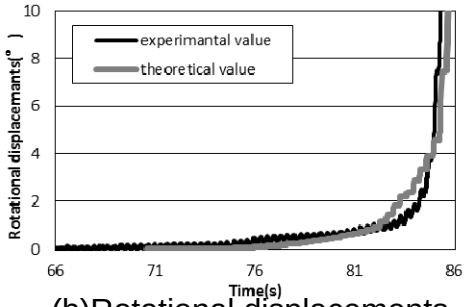


(a)Time history of input accelerations (b)Rotational displacements

Fig .11 Comparisons between experimental value and theoretical value

$(L/b=7,\theta=80°,3\text{Hz},\delta=25.7°)$

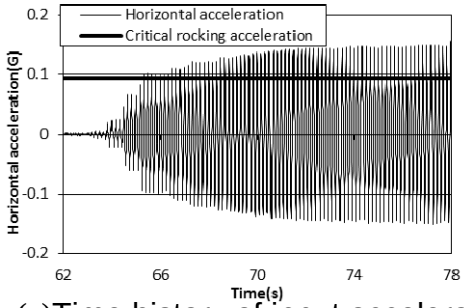


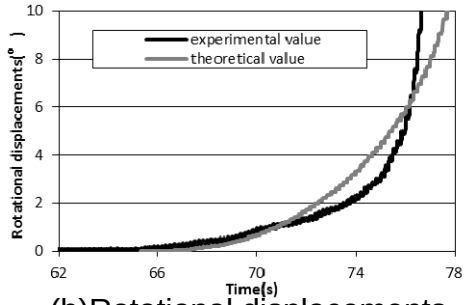


(a)Time history of input accelerations (b)Rotational displacements

Fig .12 Comparisons between experimental value and theoretical value

$(L/b=7,\theta=80°,6\text{Hz},\delta=25.0°)$

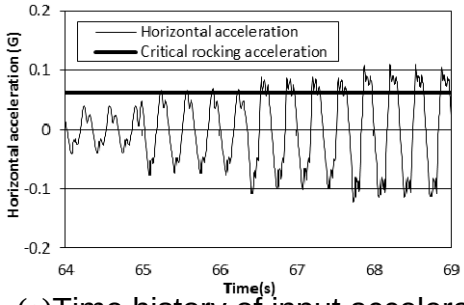


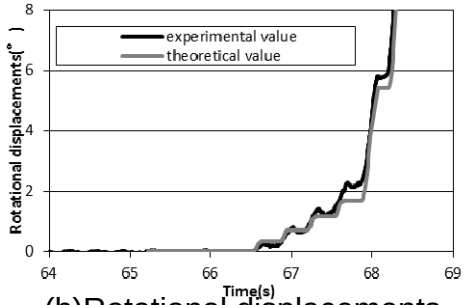


(a)Time history of input accelerations (b)Rotational displacements

Fig .13 Comparisons between experimental value and theoretical value

$(L/b=7,\theta=82°,3\text{Hz},\delta=24.9°)$

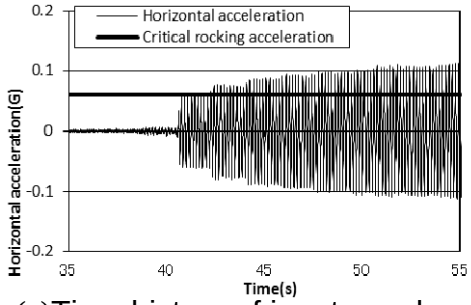


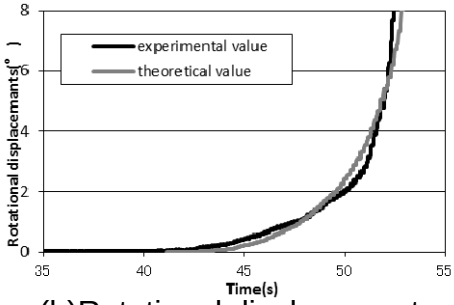


(a)Time history of input accelerations (b)Rotational displacements

Fig .14 Comparisons between experimental value and theoretical value

$(L/b=7,\theta=82°,6\text{Hz},\delta=24.3°)$

Predicted times that input accelerations exceed the critical rocking accelerations and those that rotational displacements start to increase in experiments show good correspondence in all cases. Furthermore, time histories of theoretical values of rotational displacements simulate those of experiments well. We confirm the validity of the proposed method to evaluate the amount of rotational displacement.

## 4. CONCLUSION

The following results were obtained in this study.

(1) We proposed a method to evaluate the amount of rotational displacement of the stone wall considering stone rocking during earthquake.

(2) To confirm validity of the method, shaking table tests using gravity retaining wall model are performed.

(3) The calculated rotational displacements of the model show good agreement with those of the test results, validity of the method for predicting rotational displacements of the walls is clarified.

## REFERENCES


Hiroishi, Y., Masui, T. and Yao, S. (2013), “Evaluation of rotational displacements of masonry wall, "Tsukiishibu", subjected to dynamic horizontal loading - Vibration tests of gravity retaining wall models -”, *J. Struct. Constr. Eng., AIJ,* **78**(685), 589-596 (in Japanese).

Hiroishi,Y., Masui,T. and Yao,S. (2012), “Evaluation of horizontal movements of masonry wall, “Tsukiishibu”, under dynamic horizontal load - Vibration tests of gravity retaining wall models –,” *J. Struct. Constr. Eng.*, **77**(672), 303-308 (in Japanese).

Masui, T. and Hiroishi, Y. (2012), “Evaluation of seismic performance of Japanese masonry walls of castles considering seismic energy absorption capacity”, *Proceedings of the 15th World Conference on Earthquake Engineering, Lisbon*.

Masui,T. and Yao,S. (2007), “Model tests on collapse behavior of masonry walls, “Tsukiishibu”, under long-term load,” *J. Struct. Constr. Eng.*, **619**, 89-95(in Japanese).

Matsunaga,N., Masui,T. and Yao,S. (2008), “Model tests on collapse behavior of masonry walls, “Tsukiishibu”, subjected to horizontal cyclic motions Shaking table tests of low masonry walls,” *J. Struct. Eng.*, **54B**, 29-36 (in Japanese).

Newmark,N.M. (1965), “Effects of earthquake on dams and embankment,” *Geotechnique*, **15**:**2**, 139-159.